Large-strain behaviour of Magneto-Rheological Elastomers tested under uniaxial compression and tension, and pure shear deformations

Gerlind Schubert, Philip Harrison*

School of Engineering, University of Glasgow, University Avenue, G12 8QQ Glasgow, UK

Abstract

The large-strain behaviour of Magneto-Rheological Elastomers (MREs) is characterised experimentally under uniaxial compression, uniaxial tension and pure shear deformation both in the absence and in the presence of magnetic fields. MREs are ''smart' materials that can alter their properties instantaneously by the application of external stimuli. They hold great potential for use in adaptive stiffness devices. So far, the large-strain behaviour of MREs has not been well explored, and their behaviour under pure shear deformation has not been characterised. Tests on silicone rubber based isotropic and anisotropic MREs, without and with the application of an external magnetic field have been performed in this investigation. The MR effect, defined as the increase in tangent moduli, is studied versus large engineering strain. Strains were measured optically using a Digital Image Correlation (DIC) system. Relative MR effects up to 284% were found under uniaxial tension, when a magnetic field strength of 290 mT was applied with the loading direction parallel to the direction of particle alignment.

Keywords: Magneto-Rheological Elastomers, Large-strain behaviour, Magneto-Rheological Effect, Digital Image Correlation, Pure Shear Deformation, Magnetic Induction

1. Introduction

Magneto-Rheological Elastomers (MREs) are smart materials whose properties can be altered reversibly and almost instantaneously by the application of external magnetic fields. This behaviour is caused by the interaction of micron-sized magnetisable particles dispersed in an elastomeric material. The magneto-rheological effect was first explored by Rabinow [1], working on Magneto-Rheological Fluids (MRFs). In MREs, the magnetic particles are locked in position by the solid rubber matrix. Anisotropic materials can be prepared by exposing the fluid MRE mixture to a magnetic field while curing, this forces the magnetised particles to align in chains, resulting in strong mechanical and magnetic anisotropy [2]. The first preliminary tests on MREs were performed by Rigbi and Jilken [3] and the dynamic small strain behaviour of MREs has since become a well-explored property [4, 5, 6, *i.e.*], using different types of matrix materials and magnetisable particles to manufacture the MREs. Also, the influence of several factors on the final properties of MREs, such as the strength of the magnetic field used during the manufacture of anisotropic MREs, was investigated by Chen et al. [7]. The magnetostriction [8] and the magnetic properties of MREs [9] have also been studied. In order to develop constitutive models characterising the complex behaviour of MREs, extensive experimental data derived from uniaxial and multiaxial deformation modes on the same type of material are required [10, 11, 12]. The large strain behaviour of MREs has been studied mainly under compression and simple shear [13, 14, 15, 16, 17] while, to the best of the authors knowledge the behaviour of MREs under pure shear or multi-axial deformations has yet to be investigated. So far, the variety of materials used in previous large-strain experiments makes it difficult to compare results from different investigations.

In this research work, uniaxial compression tests up to 50% strain, uniaxial tension tests up to a maximum of 100% strain and pure shear experiments up to a maximum of 70% strain were conducted to characterise both the mechanical behaviour and the MR effect of the manufactured MREs. Magnetic field strengths up to 450 mT were applied parallel to the loading direction. For anisotropic MREs, the particle alignment direction was oriented both parallel and perpendicular to the loading direction. The MR effect, defined here as the increase in tangent moduli due to the application of a magnetic field, is studied versus large strain. Together with earlier work in which MREs were studied under equi-biaxial tension up to 10% strain [18], the combined experimental data represent a comprehensive dataset essential for the development of accurate constitutive models for MREs.

*Corresponding author. Tel.: +44 141 330 4318

Email address: Philip.Harrison@glasgow.ac.uk (Philip Harrison)

2. Materials

Silicone rubber *MM 240TV* mixed with 30w% silicone oil *ACC 34*, both purchased from *ACC Silicones* were used to create the elastomeric matrix material. Carbonyl iron particles (CIP), provided by *BASF*, were used as the magnetisable particles. The average particle size ranged from 3.7 to 4.7 μm (CIP type SQ). Samples of neat rubber material together with both isotropic and anisotropic MREs, each with volume particle concentrations of 10%, 20% and 30%, were prepared. All the components were mixed thoroughly for three minutes with a hand mixer before degassing in a vacuum chamber for 10 min both before and after the mixture was poured into the moulds. The MREs were fast-cured for 1.5 hours at 100°C. To prepare anisotropic MREs, the mixture inside the moulds was exposed to 400 mT magnetic field strength during the curing process. Optical microscopy revealed uniform particle distribution in isotropic MREs and strong particle alignment in anisotropic MREs.

Cylindrical samples with a diameter of 29 mm and a height of 12.5 mm were prepared for the compression tests. Dumbbell shaped samples were manufactured with a gauge section measuring 16×4 mm, with a thickness of 2 mm, and with an overall length of 50 mm for tensile tests. Sample sheets with dimensions $50 \times 30 \times 1$ mm were manufactured in moulds for the pure shear experiments. The dimensions of the MRE samples tested are in accordance with the *British Standards* [19, 20, 11]. All moulds used to prepare samples were made of aluminium and brass to avoid any unwanted magnetisation of the moulds during the manufacturing process.

3. Test Setup and Procedure

Large-strain experiments on both isotropic and anisotropic MREs with 0, 10, 20, and 30 vol% iron content have been conducted. The experiments were carried out using a *Zwick Z250* uniaxial test machine equipped with a 250 kN load-cell in the case of compression tests, whereas a 1 kN load-cell was used for the other tests. Bespoke test rigs were designed for each of the experiments, enabling the use of strong permanent magnets (*Neodymium N52*), which were used to induce magnetic fields during the tests. The dimensions of the permanent magnets were $50 \times 50 \times 25$ mm. The top and bottom magnets remained stationary, while the crosshead of the test machine was moved; consequently the distance between the magnets remained fixed throughout the tests, ensuring a relatively constant magnetic flux density (though small changes were inevitable due to the changing shape of the test specimens) and reducing the influence of a changing attractive force between the magnets during the tests. All test-rigs were built using non-magnetic materials (aluminium and brass). The magnetic flux was measured experimentally with a *Gaussmeter* (Model 5180 from *F.W. Bell*), and the distribution and level of the magnetic flux density was simulated using the multi-physics commercial finite element software *Comsol*. All tests were displacement controlled. Where possible, strains were measured optically using *Digital Image Correlation* (DIC). The *Limess* DIC system consisting of two high-resolution cameras (4M $pixels$) able to record up to 15 frames per second, two lights, and the software *VIC-3D* were used. To facilitate DIC measurements, samples were sprayed with a white paint random speckle pattern, and a series of images was taken during the tests.

The MRE materials are sensitive to stress softening, a well-known effect in rubber-like materials known as the *Mullins* effect [21]. A comprehensive review of the *Mullins* effect is provided by Diani *et al.* [22]. The highest stresses occur in the first loading cycle, but are much lower in subsequent cycles. After the first cycle the samples retain a remnant deformation, which can be either permanent or temporary or a combination of both. The strain level that samples experience in the first cycle is called the 'preconditioning strain'. Note that the preconditioning strain has been found to be of great importance for the material's subsequent mechanical behaviour. Preconditioning a sample up to a larger strain results in a softer material, and as soon as the material is tested up to new larger strain levels its properties significantly change once again [10]. Note that the *Mullins* effect is also time-dependant, so when repeatedly testing the same MRE specimen, given enough time between tests, the stress softening again becomes apparent. In order to mitigate the influence of the *Mullins* effect, a four-cycle test procedure was performed. The third loading cycle was consistently used to characterise the material while the fourth cycle was performed merely to check that no further significant changes occurred after the third cycle. To characterise the response of the MRE material both in the absence and in the presence of magnetic fields, a minimum of three distinct testing steps were conducted, each step consisting of four loading-unloading cycle tests. The MRE samples were re-used in each subsequent step in the test series. In general, the test series consisted of three test steps:

(i) Tests in the absence of a magnetic field (*NoField01*)

(ii) Tests with different levels of magnetic field strength

(iii) Repetition of the no-field tests (*NoField02*)

However, in the tension experiments, additional test steps were introduced to examine issues such as stress-softening and damage. Measurements of sample dimensions were repeated before each testing step to detect any permanent deformation that may have occurred during the previous test. Re-using the samples could introduce possible viscoelastic creep and relaxation effects into the experimental data that cannot simply be eliminated by a preconditioning process. The behaviour of MREs is very complex and isolating any of those effects is extremely difficult. Therefore, the *NoField02* tests were performed to identify any divergence with the first set of no-field test results, *NoField01*. The aim was to ensure the results used

to evaluate the MR effect were free of the Mullins effect and also free of any other possible viscoelastic creep effects. The goal was to ultimately reveal the true nature of any MR effect.

Compression Tests. Uniaxial compression tests were performed in accordance with the *British Standard* [19]. Tests were carried out using a test speed of 10 mm/min. Samples were compressed up to 6.5 mm; equivalent to 50% engineering strain. The polished aluminium plates of the setup were lubricated. Four repeat tests on each type of MRE (both isotropic and anisotropic, each with different amounts of iron particles) were conducted, re-using the samples in each test step, including tests: (i) without a magnetic flux (*NoField01*), (ii) with a magnetic flux of 450 mT (created with an inter-magnet distance of 35 mm), (iii) with a magnetic flux of 210 mT (created with 62 mm distance between the magnets), and (iv) without magnetic flux (*NoField02*). The compression test setup with the permanent magnets in place is illustrated in Figure 1.

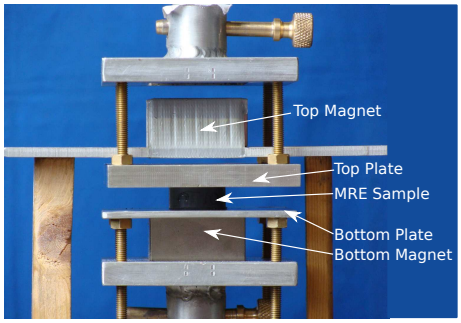

Figure 1: Test setup for the compression tests with an inter-magnet distance of 35 mm creating 450 mT magnetic induction. The magnets remained in a fixed position during the tests.

Tension Tests. Uniaxial tension tests at a test speed of $50mm/min$ were performed up to 15%, 50%, 75% and 100% strain to investigate the stress-softening present in MRE samples. Overall, a series comprised of six different testing steps were performed, including: (i) preconditioning of the samples with fifty cycles, (ii) tests without a magnetic field (*NoField01*), (iii) tests with an average applied magnetic induction of 220.6 mT (using an inter-magnet distance of 89 mm), conducted up to a maximum of 100% strain, (iv) tests with an average magnetic induction of 251.2 mT (using an inter-magnet distance of 73 mm), conducted up to a maximum of 50% strain, (v) tests with an average applied magnetic induction of 289.2 mT (using an inter-magnet distance of 63 mm), conducted up to 15% strain, and (vi) tests without a magnetic field (*NoField02*). The maximum strains mentioned above were restricted, as higher magnetic inductions required lower distances between the permanent magnets and, consequently, due to the nature of the test setup, lower tensile strains were possible. The test setup both without and with magnets in place is illustrated in Figure 2. Also shown are the cameras of the DIC system used to measure the strains. The distribution of the magnetic flux

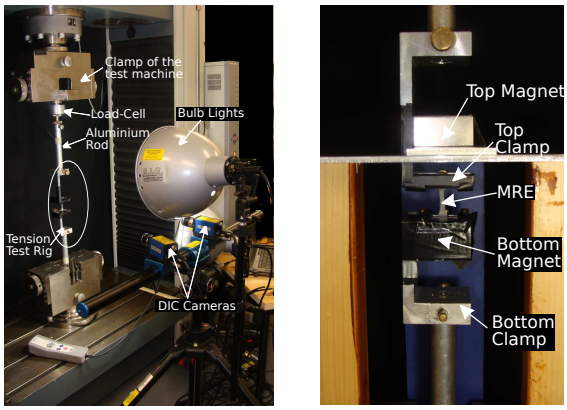

Figure 2: Test Setup for uniaxial tension tests is shown (a) with the DIC system (parts of the setup are covered in black tape to avoid reflection), and (b) the magnetic setup with an inter-magnet distance of 73 mm producing 251.2 mT.

density in each setup, calculated with the multi-physics software *Comsol*, is illustrated in Figure 3. The flux is not

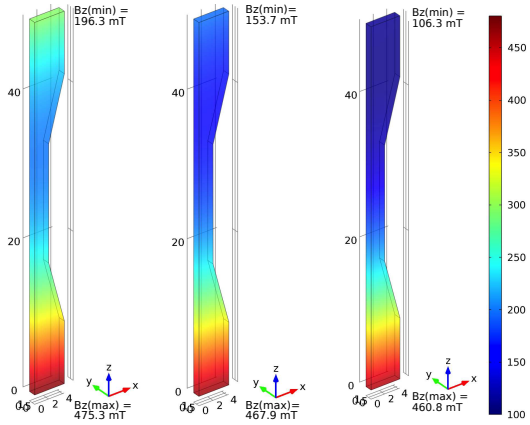

(a) 289.2 mT (b) 251.2 mT (c) 220.6 mT

Figure 3: Distribution of the magnetic flux density B_Z within the MRE sample ($\mu_r = 1$). Simulation results of all magnetic setups are illustrated as volume plots. Symmetry conditions were applied.

uniformly distributed due to the large distance between the magnets. The minimum and maximum values of the magnetic flux acting within the region occupied by the MRE samples are provided in Figure 3.

To exclude damage of the MRE sample due to large tensile strains, fatigue tests were carried out in advance to the experimental test series described in this article. Therefore MRE tension samples were tested up to a set displacement over 100 loading and unloading cycles. The stress softening versus cycle number was studied and a sample was considered as being stable when the relative tensile load no longer decreased during continued loading cycles. In the experiments presented here, the MRE samples were not tested to strains over these predetermined 'stable strain limits'.

Pure Shear Tests. Pure shear experiments were performed at a test speed of 50 mm/min up to 45% strain. The pure shear experiment is basically a 'very wide tensile test' [10], but due to the incompressibility of the material 'a state of pure shear exists at a 45 degree angle to the stretching direction' [10]. To achieve the state of pure shear, a thin strip of rubber is required; "the height of the strip in the straining direction should be no more than one-fifth of its longest dimension" [11]. The sample width was restricted to 50 mm, and the thickness of the sample was set at 1 mm since thinner samples were difficult to manufacture. The height was set at 30 mm, leading to a free height between the testing clamps of about 12 mm. The final ratio between height and width of the sample was 1/4, slightly less than the recommended ratio given in the *British Standard* [11], but still acceptable as experimental strains measured in the horizontal direction were small (ideally these should be zero). Overall four repeat tests on each type of MRE were conducted re-using the samples, including tests: (i) to precondition the samples using over 50 cycles at a test speed of 200 mm/min, (ii) without a magnetic flux (*NoField01*), (iii) with a magnetic flux density of 290 mT (using a distance between the magnets of 53 mm), and (iv) without a magnetic flux (*NoField02*).

4. Method of Analysis

The test machine recorded four-cycle load-displacement data. The third loading cycle of those data was extracted and shifted to zero displacement. To do so the remnant deformation was determined manually by examining the change of slope of the load-displacement data. Engineering stresses were calculated with the reference area (original dimensions), determined using three measurements taken on each sample. In the case of compression samples, engineering strain values were calculated using the original height of the samples. In the case of tension and pure shear experiments engineering strains were obtained with the DIC system as detailed in Section 5.1. To interpret the non-linear stress-strain behaviour of MREs the tangent moduli, E_T, was calculated as the linear slope using 1% strain increments. Use of this small increment makes this a reasonable approximation of the first derivative of the stress-strain curves. Magneto-Rheological (MR) effects are characterised by comparing the stress-strain curves resulting from tests conducted both with and without magnetic fields. The absolute MR effect is defined as the difference between the moduli E_M and E_0 of tests with and without magnetic induction.

$$\mathrm{MR}_{abs} = E_M - E_0 \tag{1}$$

The relative MR effect is defined as the factor between the moduli:

$$\mathrm{MR}_{rel} = E_M/E_0 \tag{2}$$

This can also be expressed as a relative increase $(E_M/E_0 - 1) \times 100$, defined here as a percentage value. MR effects, calculated using E_T, are plotted versus large engineering strain in the figures in Section 5.4 (smoothed using the moving average method involving a span of 10).

To achieve statistically reliable experimental results, at least three samples of the same type were tested, mean values and standard deviations of the third loading cycle are used to present stress-strain results and are used to calculate the no-field moduli and MR effects.

5. Results

5.1. DIC Measurements

The *Digital Image Correlation* (DIC) system *Limess* was used to measure the strains in uniaxial tension and pure shear tests. Tests were sprayed with a white random speckle pattern. Figure 4a shows a pure shear sample prepared for strain measurement using DIC. Grid lines were also drawn on the sample to enable calculation of the strains by measuring *pixel* positions. A series of images was recorded during the cyclic tests. The DIC software *VIC-3D* performed correlation analysis by comparing the defined Area of Interest (AoI) in each image. The software divides the pattern into smaller areas and follows the same areas of the pattern in each image. During the test, the speckle pattern is stretched and displaced. By tracking the speckle pattern, the DIC software is able to calculate the displacements and strain across the test sample. Figure 4b shows the vertical displacement across the AoI of an isotropic pure shear sample containing 20% iron content when tested up to 6 mm displacement. The calculated displacements within the AoI range from 1.32 mm to 4.02 mm, which is reasonable since the AoI is not defined from the bottom to the top clamp (in order to exclude possible boundary effects). The output of the DIC software are matrices containing values of displacement and engineering strain in both the vertical and horizontal directions at each point in the AoI at any given time. Confidence values describing the match at each point are also provided. DIC data have been post-processed using *Matlab* and confidence values are used to eliminate unreliable strain results, and thus to reduce the size of the AoI. Mean values and standard deviations are calculated from the remaining AoI and are plotted versus time in Figure 5. As a representative example, the results of an isotropic MRE

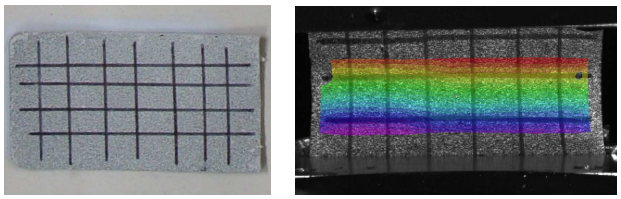

Figure 4: (a) Pure shear sample prepared for optical strain measurement, and (b) the displacement field, calculated by the DIC system, at maximum displacement (6 mm) of an isotropic 20% MRE, is shown. The vertical displacement ranges from 1.32 mm to 4.02 mm.

containing 30 *vol*% iron particles tested up to 50% tensile strain are presented. Similar data could be presented

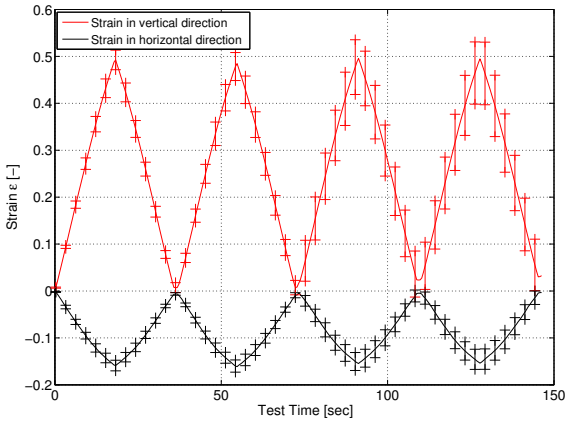

Figure 5: Mean values and standard deviation of the strain in vertical and horizontal direction versus time calculated by the DIC software *VIC-3D* and post-processed with *Matlab*. Results of an isotropic MRE with 30% iron content tested up to 50% tensile strain are shown as a representative example.

from the pure shear experiments, although here horizontal strains are much smaller, at around 2% when a pure shear sample is stretched up to 30% vertical strain.

The load versus displacement data recorded by the test machine are connected to the strain-time data of the DIC analysis via the time recorded by the test machine.

5.2. Discrepancies between No-Field Tests

In each of the large-strain experiment tests conducted in the absence of an applied magnetic field were repeated at the end of the test series (see Section 3) to check whether or not the stress-strain results were in agreement. In the case of compression and tension tests discrepancies between *NoField01* and *NoField02* tests were found. The stress-strain curves diverge after a certain level of strain as shown in Figure 6. The *NoField02* resulted in lower stresses, indicating increased stress-softening compared to the *NoField01* tests. Divergence points, defined as the strain values where the absolute difference between two mean curves become larger than the associated standard deviations, are indicated with arrows in Figure 6. The divergence points of both the uniaxial compression and tension tests of all types of MREs are summarised in Table 1. Stress-strain results of the pure shear *NoField01* and *NoField02* tests did not diverge.

In both the compression and tension test specimens, permanent deformations were found, whereas the pure shear specimens recovered quickly to their original dimensions between each of the tests, due to their lower thickness. The permanent deformation present in compression and tension samples led to higher strain levels in the subsequent tests and, consequently, due to the *Mullins* effect, to differences in the stress-strain results. To eliminate this effect and to ensure analysis of reliable experimental data,

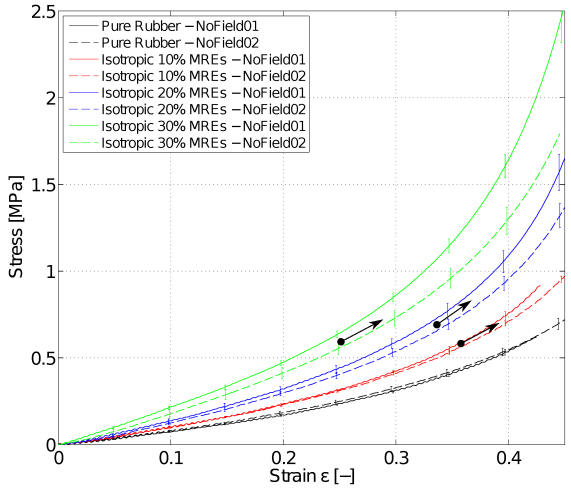

Figure 6: Stress-strain curves from *NoField01* and *NoField02* compression tests of pure rubber and isotropic MREs with 10% to 30% iron content. The arrows indicate the divergence points.

MRE Sample	Iron [%]	Divergence Point = Strain Value [–] Compression	Tension
Pure Rubber	0	no separation	no separation
Isotropic MREs	10	0.36	0.42
	20	0.34	0.19
	30	0.25	0.19
Vertically aligned MREs	10	0.28	0.26
	20	0.26	no separation
	30	0.16	0.31
Horizontally aligned MREs	10	no separation	0.35
	20	0.35	0.29
	30	0.27	0.06

Table 1: Comparison between *NoField01* and *NoField02* compression and tension tests (up to 50% strain). The divergence points, defined as the strain values where the absolute difference between two mean curves become larger than the associated standard deviations, are listed.

the MREs were characterised using stress-strain data only up to the point of divergence. Note that in future applications, MREs are likely to be 're-used' and permanent deformations are, therefore, likely. It is recommended that MRE samples are preconditioned up to strain levels higher than those planned during the working operation of the MRE application.

In the remaining part of this article, results of the *NoField02* tests are considered and bold lines are used to represent the MR effects only up to the point of divergence.

5.3. No-Field Moduli

Both the increase in stiffness and stress due to higher particle concentration in the elastomer and due to the particle alignment were studied. The stress-strain curves of all MREs tested under compression, tension and pure shear, in the absence of a magnetic field are illustrated in Figure 7. Clearly, all types of MREs show strongly non-linear

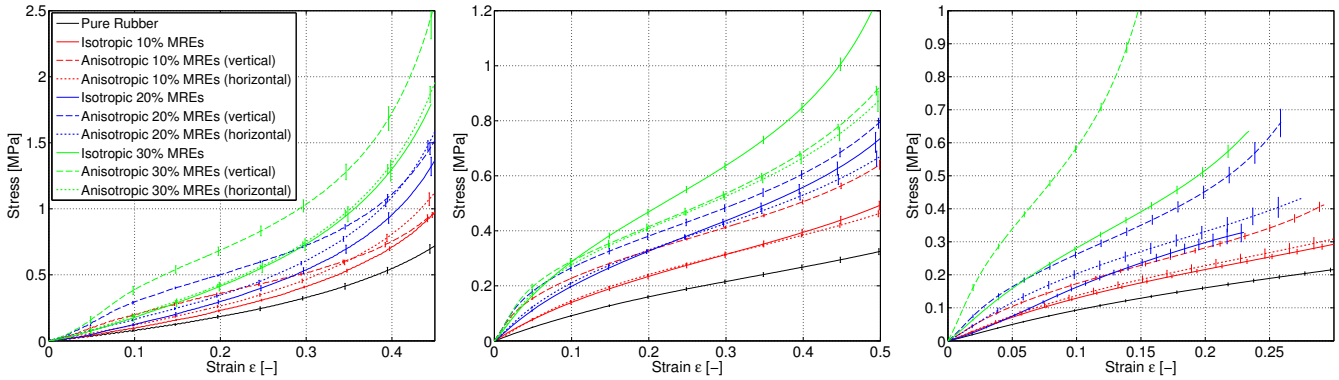

Figure 7: Stress-strain results of (a) compression up to 50% strain, (b) tension up to 50% strain, and (c) pure shear tests up to 45% strain in the absence of a magnetic field of pure rubber, isotropic, and anisotropic MREs with 10% to 30% iron content are illustrated. The legend in Figure 7a is valid for all plots illustrated.

stress-strain behaviour. Anisotropic samples with vertical particle alignment exhibit the highest stresses and moduli. Results start with a steep slope that flattens from approximately 10% strain and increases again above 30% strain; this trend is independent of particle content. Isotropic and anisotropic MREs with horizontal particle alignment show a very similar stress-strain curve shape with constantly increasing slope, although the isotropic MREs exhibit slightly lower stresses. An exception to this is the MRE with 30% iron content, tested under uniaxial tension; here the isotropic samples clearly exhibit larger stresses in the large-strain region than either of the anisotropic MREs. There is some uncertainty whether this is a real effect or spurious experimental data; the reasons are not yet clear. Higher volume particle concentrations lead to higher stresses; this is true for all types of MRE samples. Note that pure shear samples (all preconditioned to 45% strain) experienced large temporary remnant deformation during the four-cycle tests, and this was far larger for anisotropic MREs with high iron content compared to isotropic MREs with low iron content, resulting in different strain levels observed in Figure 7c. Tension tests were performed up to different strain levels. MRE samples preconditioned and tested up to higher strains are apparently softer than the same type of MRE tested to lower strain levels. The stress softening is more pronounced in anisotropic MREs and in MREs with high iron contents.

To interpret the non-linear stress-strain curves, the tangent moduli, E_T, was calculated and the values between 1% and 2% strain (where the largest MR effect usually occur) are compared for each of the deformation modes, and for each type of MRE in Figure 8. The moduli represent results collected during tests up to 50% compressive strain, 50% tensile strain and 45% strain in pure shear. The moduli of MREs under compression are the lowest, and those under pure shear deformation are the highest. The moduli were found to increase with increasing iron content; the increase was found to be almost linear in the case of uniaxial tension tests, while in the other large-strain experiments

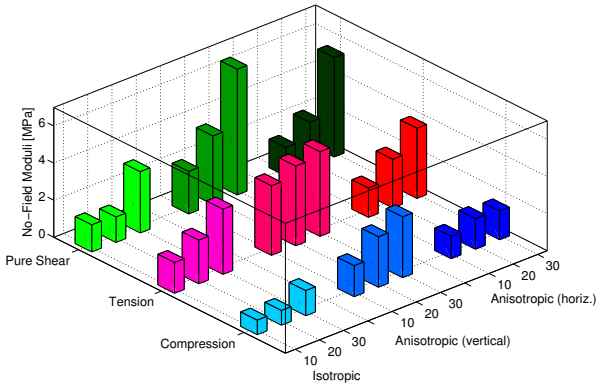

Figure 8: Comparison of the mechanical response for all deformation modes and all types of MREs with particle concentrations from 10% to 30%. The tangent moduli between 1% and 2% strain are illustrated.

the modulus of MREs containing 30% iron volume fraction exceeded the linear trend.

5.4. MR Effect

To study the influence of the magnetic field, the stress-strain results conducted from both tests in the absence and in the presence of magnetic fields were studied. The relative MR effects as defined in Equation 2 were determined using the resulting data.

Compression Tests. Compression tests with two different magnetic field strengths, 450 mT and 210 mT, were performed to measure the MR effect. Figure 9 compares the stress-strain curves of the no-field tests and the magnetic tests with 450 mT magnetic field strength. The relative MR effects are illustrated versus strain in Figure 9d. In most samples, an increase in stress is observed due to an applied magnetic flux. The MR effect increases with increasing iron content, with the vertically aligned anisotropic samples achieving the highest relative MR effects. Most of the curves in Figure 9d start with high effects in the small-strain region that decrease to nearly

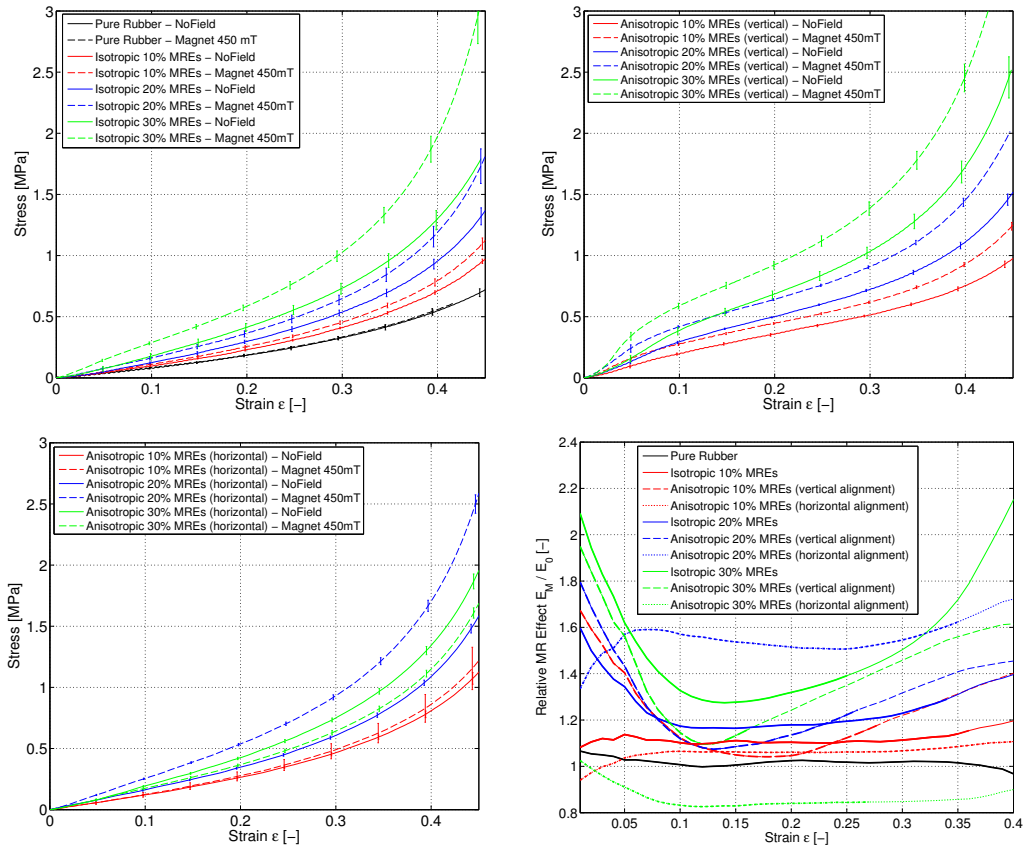

Figure 9: Stress-strain results of the uniaxial compression tests without and with an applied magnetic field strength of 450 mT (a-c), and the relative MR effects are compared (d). Bold lines represent the parts up to the divergence points.

no effect in the mid-strain region, although, surprisingly, the effect increases again at strains greater than 15%. As expected, pure rubber samples exhibit no noticeable MR effect, and effectively serve to verify that the experimental setup is reliable; the relative MR effect measured using the pure rubber samples indicates an experimental error of about 6.6%. Anisotropic MREs with 30% vertically aligned particles exhibit the highest MR effects, with an absolute increase in modulus of 3.65 MPa; over twice as stiff in the presence of a magnetic field as without. Interestingly, the anisotropic MREs with horizontal particle alignment exhibit nearly no MR effect and start with a decreased stiffness in the small-strain region. Only the anisotropic MREs with horizontal particle alignment containing 20% CIP exhibit a significant relative MR effect of 59%, but the curve shape of the MR effect versus strain is different compared to other curves; the effect occurs at 7% strain. The relative MR effects achieved in the small-strain region of both magnetic tests are plotted versus the volume particle concentration in Figure 10. The MR effect increases with increasing volume particle concentration and the MR effect of anisotropic MREs is higher than that of isotropic MREs. The model presented by Davis [23] predicts a non-linear relation between MR effect and volume particle concentration with a maximum MR effect at 27% iron content. Based on the limited number of experimental data points presented here, firm conclusions in this regard are not possible. The MR effect increases approximately linearly with increasing applied magnetic field strength, which is not explicitly illustrated for the

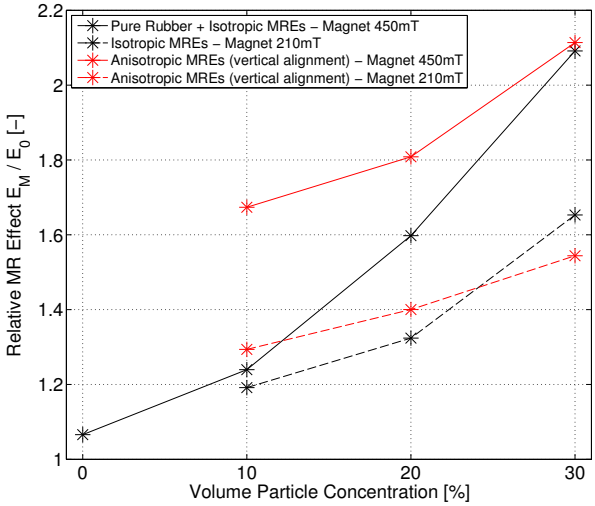

Figure 10: MR effects achieved in compression test with 450 mT and 210 mT magnetic field strength are illustrated versus the volume particle concentration.

compression tests but can be derived from Figure 10.

Tension Tests. Three different magnetic field strengths, on average 289.2 mT, 251.2 mT, and 220.6 mT, were applied to determine the response of the MRE materials. The maximum strain levels in tests involving a magnetic field were restricted due to the fixed inter-magnet distance. First, the stress-strain data of the no-field tests and that of the magnetic tests with the highest magnetic field strength of 289.2 mT are compared in Figure 11. Relative MR effects are plotted versus engineering strain in Figure 11d. Anisotropic samples with vertical particle alignment exhibit the highest MR effects, followed by the anisotropic MREs with horizontal particle alignment; whereas isotropic MREs show the lowest MR effects. Results measured using pure rubber samples indicate an experimental error of about 7.6%. All MR effects are largest in the small strain regime and decrease rapidly to nearly 1 in the mid-strain regime, but the relative effects tend to increase again for strains above 10%. The modulus of an anisotropic MRE with 30% vertical aligned particles increases by about 12.17 MPa in absolute terms, equivalent to a relative increase of about 284% (almost three times stiffer) in the small strain regime. To study the MR effects present in the large-strain region, test setups with smaller magnetic inductions of 251.2 mT and 220.6 mT have to be considered. The relative MR effects versus strain achieved in these tests are illustrated in Figure 12. As expected, the MR effects in these tests are lower than those obtained in the tests conducted using a 289.2 mT magnetic field strength. Nevertheless, in Figure 12 it can be seen that the MR effects increase in the large-strain region above 15% strain and, in the case of MREs containing 10% iron particles, the MR effects at large strain exceed the MR effects present at small strains.

As noted in Section 5.3, the no-field moduli are smaller when samples are preconditioned and tested up to a higher strain level. MR effects present in the small-strain region measured with a 289.2 mT magnetic flux are illustrated versus the preconditioning level in Figure 13a. Clearly, MREs show a higher MR effect when the samples were preconditioned to a larger strain level. This effect is more pronounced in the case of anisotropic MREs with vertical particle alignment. This observation leads to the conclusion that preconditioning samples to the highest possible strain level enhances the MR effect. The MR effect present in the small-strain region increases linearly with increasing applied magnetic flux density, this is illustrated for samples preconditioned up to 50% strain in Figure 13b.

Pure Shear Tests. In the pure shear test series, only one magnetic field strength of 290 mT was applied to study the MR effect. Stress-strain curves comparing the results of no-field and magnetic field tests are illustrated in Figure 14. The relative MR effects are plotted versus engineering strain in Figure 14d. The highest MR effect of 2.05 MPa (absolute) and 57% (relative) was achieved with the anisotropic MREs with 20% vertically aligned particles. MREs with 30% iron content did not show high MR effects, likewise for anisotropic MREs with horizontal particle alignment. The MR effect measured on pure rubber in the small strain region indicated an experimental error of about 20%, which is large compared to the errors found in compression and tension tests. The relatively small MR effects and the large experimental error might be due to the non-uniformity of the magnetic flux density in pure shear experiments (predicted by the *Comsol* simulations of the magnetic field). Horizontal strains up to 2% were measured, but ideally no horizontal strains should occur to achieve a state of pure shear. This could also cause experimental errors.

Comparison of Deformation Modes. In all experiments, the largest MR effects occurred in the small-strain region. The relative MR effects are summarised in Table 2, and are illustrated in Figure 15. To enable comparison, the relative MR effects are related to a 100 mT applied magnetic field strength. The highest MR effects were achieved

MRE Sample	Iron [%]	Relative MR Effect E_M/E_0 Compression	Tension	Pure Shear
Pure Rubber	0	1.07	1.08	0.99
Isotropic MREs	10	1.24	1.12	1.10
	20	1.60	1.21	1.49
	30	2.09	1.29	1.15
Vertically aligned MREs	10	1.67	2.23	1.44
	20	1.81	3.08	1.57
	30	2.11	3.84	1.19
Horizontally aligned MREs	10	1.07	1.27	1.08
	20	1.59	1.52	1.12
	30	1.02	2.21	1.27

Table 2: Relative MR effects of isotropic and anisotropic MREs tested in uniaxial compression with 450 mT flux density, in uniaxial tension with 289.2 mT induction, and in pure shear deformation with 290 mT flux, are listed.

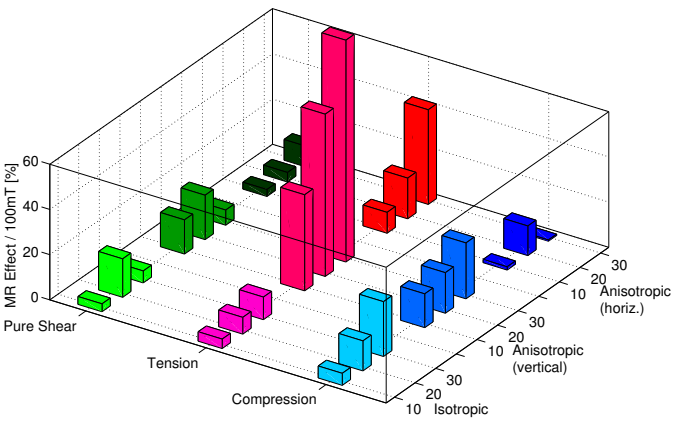

Figure 15: Comparison of relative Magneto-Rheological (MR) response for all deformation modes, and all types of MREs with particle concentrations from 10% to 30%. The MR effects are related to 100 mT applied magnetic flux density.

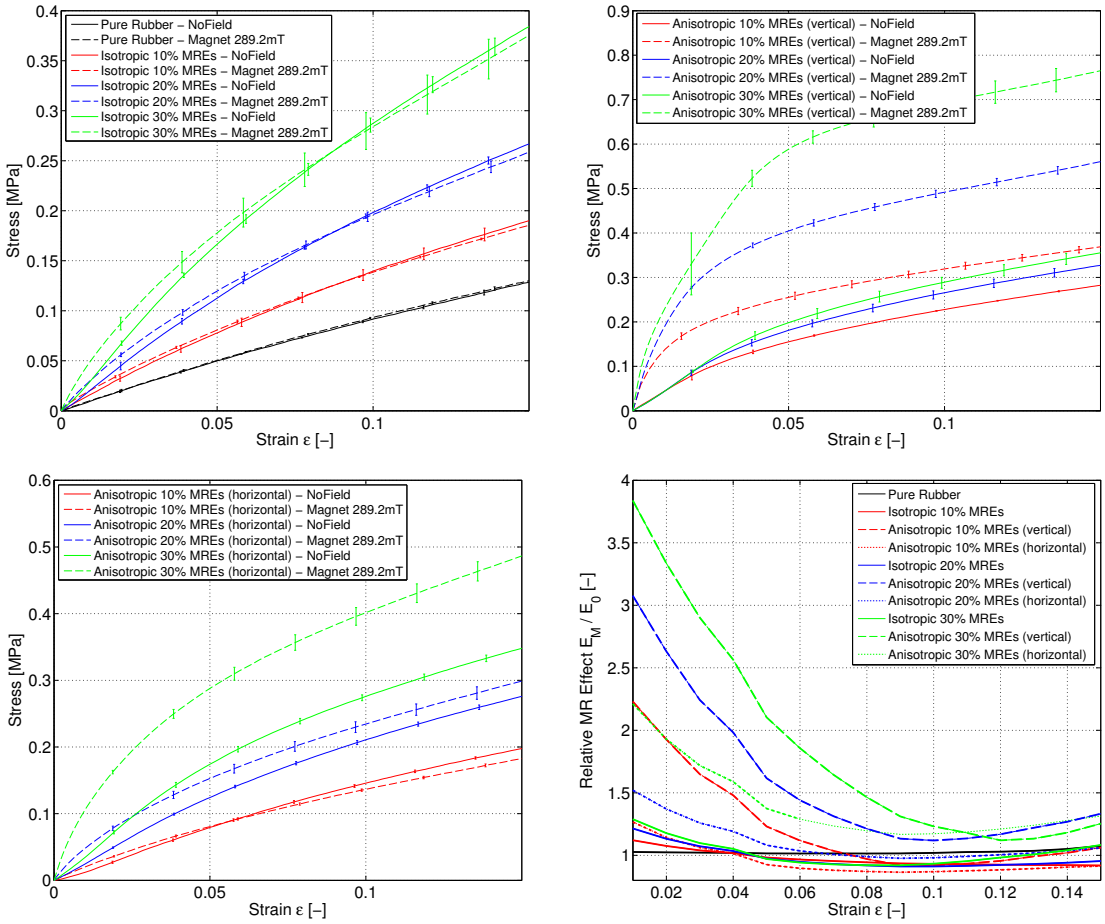

Figure 11: Stress-strain results of the uniaxial tension tests (samples preconditioned to 50% strain) without and with an applied magnetic induction of 289.2 mT are illustrated (a-c), and the relative MR effects are compared (d). Note that the strain was restricted to 15% due to the inter-magnet distance. The MR effects are calculated with the tangent moduli using 1% stress-strain increments, and the curves are smoothed with the moving average method using a span of 10. The bold lines represent the parts up to the divergence points.

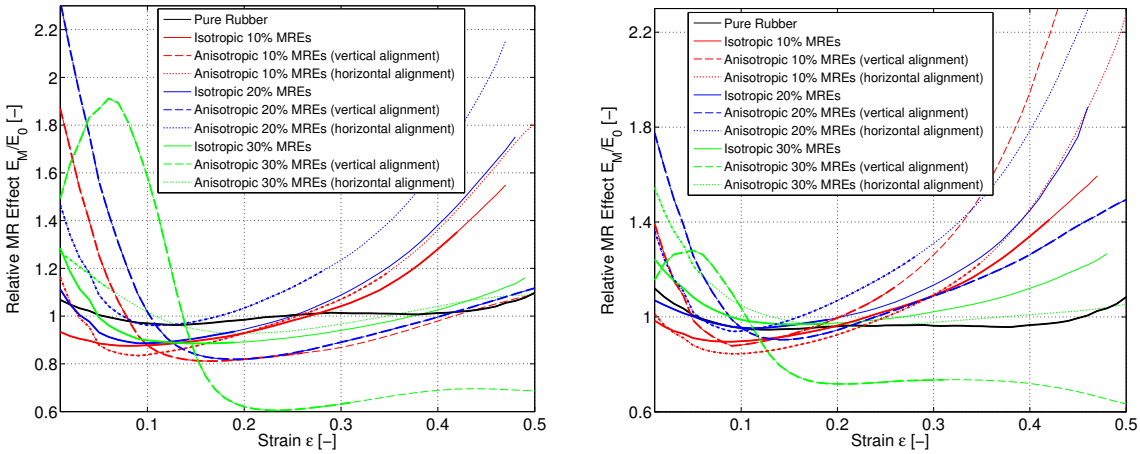

Figure 12: The relative MR effect of MREs preconditioned to 50% strain in uniaxial tension tests with applied magnetic inductions of 251.2 mT (a) and 220.6 mT (b) are illustrated. The MR effects are calculated with the tangent moduli using 1% stress-strain increments, and the curves are smoothed with the moving average method using a span of 10. The bold lines represent the parts up to the divergence points.

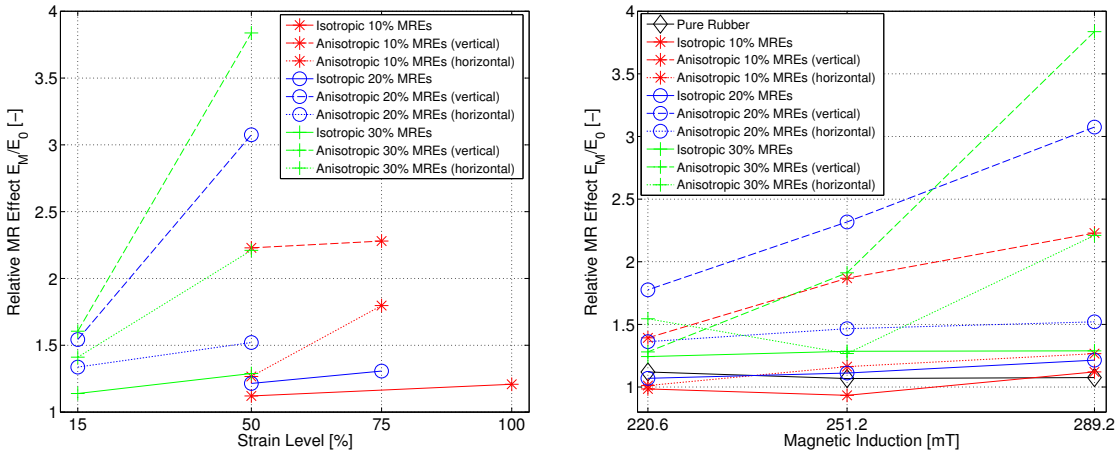

Figure 13: Relative MR effects achieved in tension are illustrated (a) versus the preconditioning level (289.2 mT magnetic field strength), and (b) versus the average magnetic flux density (MREs preconditioned to 50% strain). The largest MR effects present in the small-strain region are illustrated.

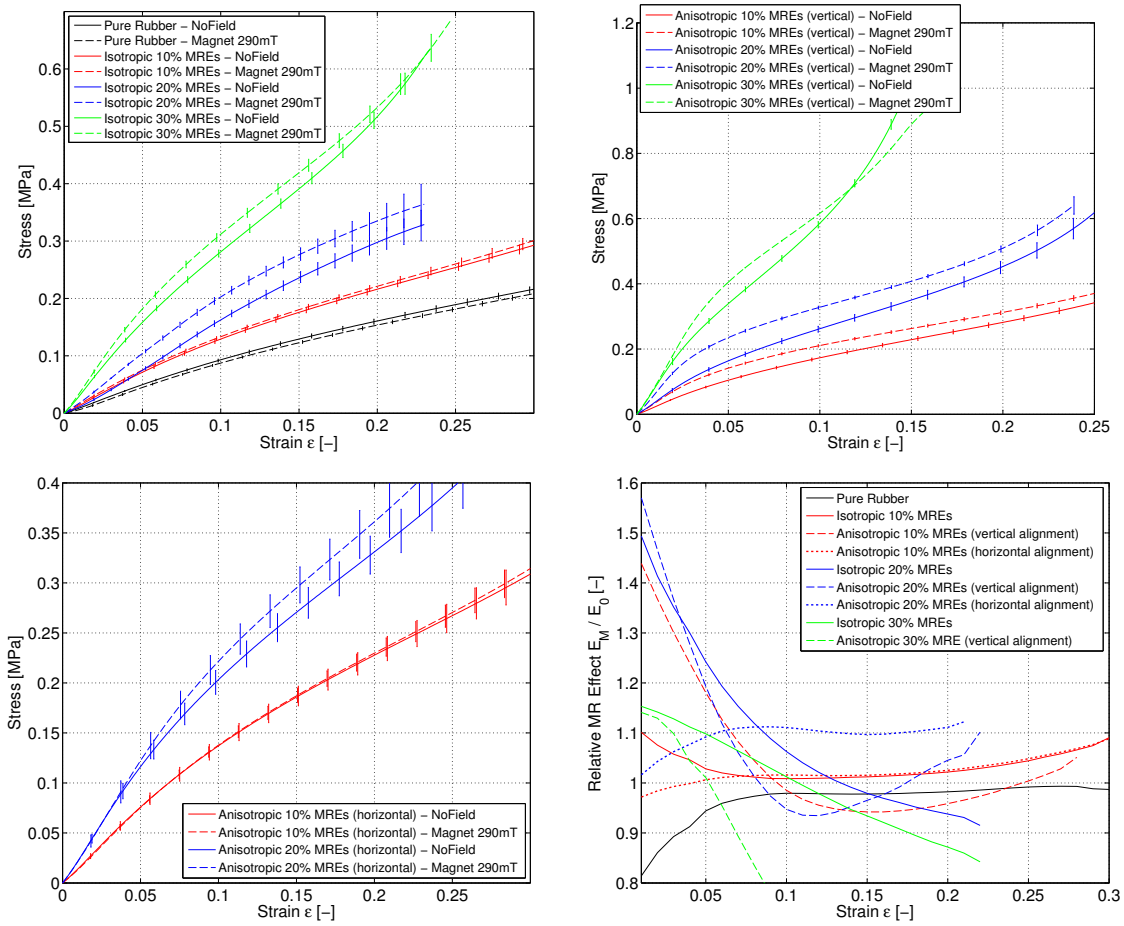

Figure 14: Stress-strain results of the pure shear tests without and with an applied magnetic induction of 290 mT are illustrated (a-c), and the relative MR effects of all types of MREs are compared (d). The MR effects are calculated with the tangent moduli of 1% strain increments, and the curves are smoothed with the moving average method using a span of 10.

in the uniaxial tension tests, followed by uniaxial compression tests. MR effects achieved in the pure shear tests were comparatively low. Anisotropic MREs with their particle alignment direction oriented in the same direction as the magnetic field usually exhibited the largest effects, while isotropic MREs exhibited the lowest effects. MR effects were generally found to increase with increasing iron content. The model presented by Davis [23] cannot be confirmed by the experimental data presented. A linear increase of the MR effects with increasing magnetic field was found.

6. Conclusions

The behaviour of silicone-rubber based MREs with carbonyl iron as the magnetic particles were studied under large strain under compression, tension and pure shear deformations. Different iron particle contents, in both isotropic and anisotropic MREs, were tested. Magnetic flux densities applied in the loading direction were created with permanent magnets. For anisotropic MREs, samples were tested both parallel and perpendicular to the particle alignment direction. In tension tests, the samples were stretched up to different strain levels to study the influence of the stress-softening *Mullins* behaviour on the MR effect. The MR effect was studied versus engineering strains, characterised using the tangent moduli calculated using 1% strain increments. Usually, the MR effects were largest in the small-strain region, but in the case of tension tests the MREs with 10% iron particle content exhibited larger MR effects in the large-strain region. MR effects were studied as a function of particle volume concentration, using different applied magnetic field strengths and different preconditioning levels. MR effects increased with increasing iron contents and MREs with vertically aligned particles usually achieved the highest MR effects. These MR effects increased approximately linearly with increasing magnetic field strength. MREs were very sensitive to the level of preconditioning strain, and revealed larger MR effects when preconditioned and tested up to larger strains. The highest MR effect was found under uniaxial tension, where the anisotropic MREs with 30% iron volume fraction exhibited a 284% relative increase in moduli, almost three times stiffer than in the no-field state.

An extensive set of experimental data has been presented in this work. Uniaxial compression, uniaxial tension and pure shear experiments were all conducted on the same type of MRE material preconditioned to similar levels of strains. The experimental data will be used in future work to evaluate hyperplastic constitutive models describing MRE materials both in the absence and in the presence of magnetic fields. This is the first experimental data set published in the literature that encompasses several different experimental deformations conducted on the same type of MRE material.

7. Acknowledgement

The project was funded by the *Glasgow Research Partnership in Engineering* (GRPE). The DIC system was loaned by the *Engineering and Physical Sciences Research Council* (EPSRC).

References

[1] J. Rabinow, The magnetic fluid clutch, in: American Institute of Electrical Engineers, volume 67, 1948, pp. 1308–1315. doi:10.1109/T-AIEE.1948.5059821.

[2] M. Jolly, J. Carlson, B. Munoz, T. Bullions, The Magnetoviscoelastic Response of Elastomer Composites Consisting of Ferrous Particles Embedded in a Polymer Matrix, volume 7, 1996, pp. 613–622. doi:10.1177/1045389X9600700601.

[3] Z. Rigbi, L. Jilken, The response of an elastomer filled with soft ferrite to mechanical and magnetic influences, volume 37, 1983, pp. 267 – 276. doi:10.1016/0304-8853(83)90055-0.

[4] J. Ginder, M. Nichols, L. Elie, J. Tardiff, Magnetorheological elastomers: properties and applications, in: Smart Structures and Materials, 1999. doi:10.1117/12.352787.

[5] H. Böse, R. Röder, Magnetorheological elastomers with high variability of their mechanical properties, volume 149, 2009, pp. –. doi:10.1088/1742-6596/149/1/012090.

[6] O. Padalka, H. Song, N. Wereley, J. Filer, R. Bell, Stiffness and Damping in Fe,Co and Ni Nanowire-Based Magnetorheological ElastomericComposites, volume 46, 2010, pp. 2275–2277. doi:10.1109/TMAG.2010.2044759.

[7] L. Chen, X. Gong, W. Li, Microstructures and viscoelastic properties of anisotropic magnetorheological elastomers, volume 16, 2007, pp. 2645–2650. doi:10.1088/0964-1726/16/6/069.

[8] X. Gong, G. Liao, S. Xuan, Full-field deformation of magnetorheological elastomer under uniform magnetic field, volume 100, 2012. doi:10.1063/1.4722789.

[9] I. Bica, Magnetoresistor sensor with magnetorheological elastomers, volume 17, 2011, pp. 83 – 89. doi:10.1016/j.jiec.2010.12.001.

[10] K. Miller, Testing and Analysis - Testing Elastomers for Hyperelastic Material Models in Finite Element Analysis, 1999, p. 88. URL: http://www.axelproducts.com/pages/downloads.html#p1, retrieved 09/2013.

[11] BS 903-5, Physical testing of rubber - Part 5: Guide to the application of rubber testing to finite element analysis, 2004.

[12] R. Ogden, G. Saccomandi, I. Sgura, Fitting hyperelastic models to experimental data, volume 34, 2004, pp. 484–502. doi:10.1007/s00466-004-0593-y.

[13] Z. Varga, G. Filipcsei, M. Zrinyi, Magnetic field sensitive functional elastomers with tuneable elastic modulus, volume 47, 2006, pp. 227–233. doi:10.1016/j.polymer.2005.10.139.

[14] G. Stepanov, S. Abramchuk, D. Grishin, L. Nikitin, E. Kramarenko, A. Khokhlov, Effect of a homogeneous magnetic field on the viscoelastic behavior of magnetic elastomers, volume 48, 2007, pp. 488 – 495. doi:10.1016/j.polymer.2006.11.044.

[15] M. Farshad, M. Le Roux, Compression properties of magnetostrictive polymer composite gels, volume 24, 2005, pp. 163–168. doi:10.1016/j.polymertesting.2004.09.007.

[16] I. Gudmundsson, A Feasibility Study of Magnetorheological Elastomers for a Potential Application in Prosthetic Devices, Master's thesis, Faculty of Industrial Engineering, Mechanical Engineering and Computer Science, School of Engineering and Natural Sciences, University of Iceland, 2011. URL: http://hdl.handle.net/1946/10168.

[17] F. Gordaninejad, X. Wang, P. Mysore, Behavior of thick magnetorheological elastomers, volume 23, 2012, pp. 1033–1039. doi:10.1177/1045389X12448286.

[18] G. Schubert, P. Harrison, Z. Guo, The Behaviour of Magneto-Rheological Elastomers under Equi-Biaxial Tension, in: The

19th International Conference on Composite Materials, Montreal, 2013. URL: http://eprints.gla.ac.uk/85550/.

[19] BS ISO 7743, Rubber, vulcanized or thermoplastic - Determination of compression stress-strain properties, 2008.

[20] BS ISO 37, Rubber, vulcanized or thermoplastic - Determination of tensile stress-strain properties, 2005.

[21] L. Mullins, N. Tobin, Stress softening in rubber vulcanizates. Part 1. Use of a strain amplification factor to describe the elastic behavior of filler-reinforced vulcanized rubber, volume 9, Wiley Subscription Services, Inc., A Wiley Company, 1965, pp. 2993–3009. doi:10.1002/app.1965.070090906.

[22] J. Diani, B. Fayolle, P. Gilormini, A review on the Mullins effect, volume 45, 2009, pp. 601–612. doi:10.1016/j.eurpolymj.2008.11.017.

[23] L. C. Davis, Model of magnetorheological elastomers, volume 85, AIP, 1999, pp. 3348–3351. doi:10.1063/1.369682.